

## ESTIMATING METHOD FOR THE IN-SOIL DEFORMATION BEHAVIOR OF GEOGRID BASED ON THE RESULTS OF DIRECT BOX SHEAR TEST

TSUTOMU NAKAMURA<sup>i)</sup>, TOSHIYUKI MITACHI<sup>ii)</sup> and ISAO IKEURA<sup>iii)</sup>

### ABSTRACT

This paper proposes a method to estimate in-soil deformation behavior of geogrid based on the results of direct box shear tests. A series of drained direct box shear (DBS) tests were performed, consisting of two types of normal stress loading methods and a series of pull-out tests in which the space of the pull-out opening, embedded length of geogrid and conditions of in-soil end restraint were changed. Comparisons were made between the calculated in-soil deformation behavior of the geogrid based on the results of the DBS tests and that of the results observed by pull-out tests.

Based on this study, the following findings were obtained. Strength parameters corresponding to the peak or the residual states obtained from the two types of direct box shear tests almost coincide with each other. Using the method proposed in this paper with the strength parameters obtained by DBS tests, it is possible to estimate the in-soil behavior of geogrid. As the pull-out force vs. pull-out displacement relationships depend not on the conditions of in-soil end restraint of geogrid but on the normal stress exerted on the geogrid, it is important to construct a reinforced soil structure so that sufficient frictional resistance develops between soil and geogrid.

**Key words:** deformation behavior, direct box shear test, geogrid, pull-out test, reinforced soil, sand (IGC: D6/E13)

### INTRODUCTION

For practical use of geosynthetics as soil reinforcement materials, the suitability of the material should be checked by evaluating not only its mechanical properties but also soil-geosynthetics interaction properties. Links between the laboratory testing methods and modeling or designing of reinforced soil structures have been reported (e.g. Jewell, 1992; Japanese geotextile research group, 2000). For obtaining frictional properties between soil and geosynthetics in the laboratory, direct shear test and pull-out test have been frequently used. These are recognized as different type of tests due to the difference of boundary conditions (Juran et al., 1988). In many studies, the pull-out test has been performed in order to determine the in-soil deformation behavior of geogrid as a model test (e.g. Ingold, 1983; Palmeira and Milligan, 1989; Bergado et al., 1993; Hayashi et al., 1996). In these reports, the pull-out mechanism or effects of some factors affecting the pull-out test results have been clarified. However, the difficulty with the pull-out test equipment is that it is large and complicated; therefore, it is troublesome to perform the test under various conditions. Moreover, it is very difficult to perform a full scale test. Due to these difficulties, the limit equilibrium method has been used as the basis for designing reinforced soil in Japan, taking no account of relative displacement be-

tween soil and geogrid (Japanese geotextile research group, 2000). Therefore, the in-soil deformation behavior of geogrid has not been regarded as an important factor to be considered.

In these circumstances, Imaizumi et al. (1995) has reported on the comparison between pull-out test results and calculated pull-out force vs. pull-out displacement relationship obtained by taking into account the friction between soil and geomembrane. The authors have performed the direct box shear (DBS) test in terms of considering it as an element test, and have clarified the effect of the factors affecting the test results (Nakamura et al., 1999).

The present paper proposes a method to estimate the in-soil deformation behavior of geogrid based on the results of DBS test which has not yet been used for such a purpose. Moreover, a comparison between calculated in-soil deformation behavior of geogrid and that as observed by pull-out tests performed under changing conditions of geogrid length, loading stress and end restraint of geogrid is discussed.

### LABORATORY TEST

#### *Direct Box Shear Testing Method*

The direct box shear test apparatus used in this paper (Fig. 1) has a 350 mm × 350 mm size upper and lower

<sup>i)</sup> Research Associate, Tomakomai National College of Technology.

<sup>ii)</sup> Professor, Graduate School of Engineering, Hokkaido University.

<sup>iii)</sup> Professor, Tomakomai National College of Technology.

Manuscript was received for review on January 9, 2002.

Written discussions on this paper should be submitted before September 1, 2003 to the Japanese Geotechnical Society, Sugayama Bldg. 4F, Kanda Awaji-cho 2-23, Chiyoda-ku, Tokyo 101-0063, Japan. Upon request the closing date may be extended one month.

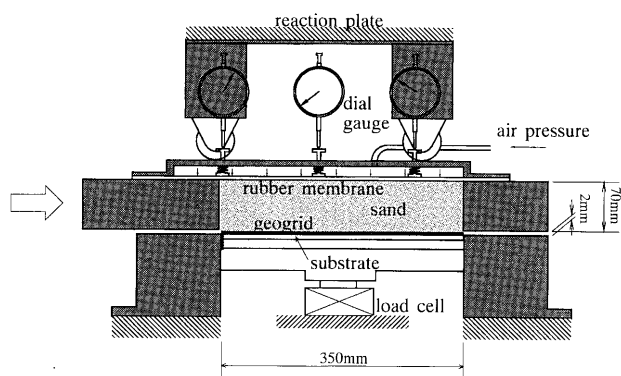


Fig. 1. Direct box shear test apparatus

Table 1. Properties of geogrid

Size (mm)			Tensile strength (kN/m)	Stiffness (kN/m)
a	b	c		
17	17	2	80	807

# tensile strength: nominal value shown in the catalogue.

# stiffness: calculated secant modulus based on the data obtained during pull-out test along the part of geogrid exposed to the air. (strain rate: 1 mm/min, temperature: 20°C)

box. This apparatus applies a vertical load at the top of the upper box using a rubber membrane with air pressure. The shear load is applied at the upper box, which is movable horizontally with a screw jack. The upper and lower boxes were made in the same size for reducing the effect of friction between the sand specimen and top surface of the lower box. Two types of normal stress loading are adopted in this study. One is the constant pressure (CP) test in which air pressure is controlled to make the normal stress on the shear plane measured by a load cell installed at the bottom of the lower box constant. The other one is the nominal constant pressure (NCP) test in which applied vertical load is kept constant. The rate of shearing is 1 mm/min and the opening between the upper and lower boxes is set up at 2 mm. The thickness of the sand layer used in this experiment is 70 mm. These values of opening between upper and lower boxes and the thickness of the sand layer are within the permissible range prescribed by ASTM D 5321-1992, JSF T 941-1994 (draft) and JGS T 0561-2000. Since the area of shear plane is decreased during shear, correction of sectional area is applied to the test results. Yufutsu Sand, whose mean diameter and uniformity coefficient are 0.29 mm and 2.8 respectively, was used. It was prepared over a geogrid installed in the direct shear box by the multiple sieve pluviation method (letting sand fall through some sieves) to give a relative density ( $D_r$ ) of 85%. A woven polyester geogrid (Fig. 2), whose properties are listed in Table 1, was used. To carry out the series of direct box shear tests, the geogrid specimen was glued to the perspex plate installed at the sliding interface. For the use of DBS test as an element test having a single side surface of geogrid material and simulating the mechanism of the pull-out phenomenon, the

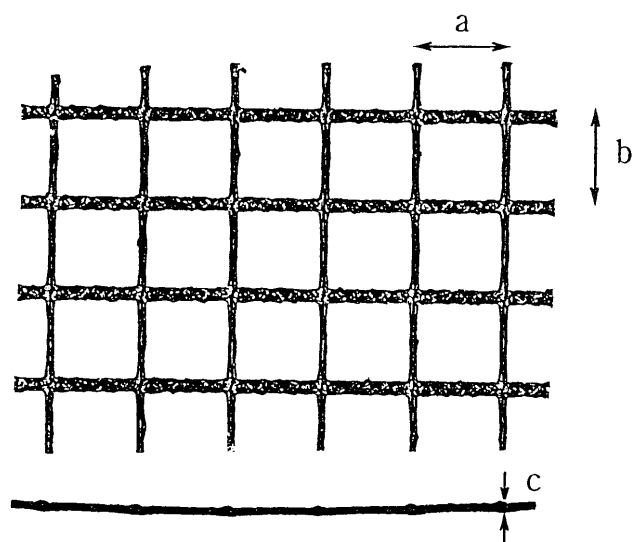


Fig. 2. Geogrid used for tests

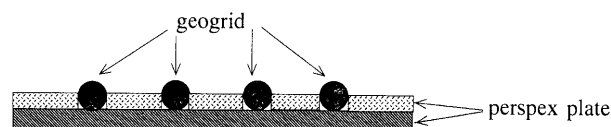


Fig. 3. Geogrid specimen for DBS test

depth of the apertures of geogrid were made to be half by putting small perspex plates, whose thickness was equal to half of the geogrid ribs, into apertures as shown in Fig. 3.

#### Results of Direct Box Shear Test

The shear stress vs. normal stress relationships from the test results of constant pressure (CP) direct box shear tests where the normal stress is controlled at a constant and nominal constant pressure (NCP) tests, in which applied normal load is kept constant, are shown in Fig. 4. Prescribed normal stresses of 25, 49, 74 kPa were initially applied in each test. The stress paths for the CP test in Fig. 4 are almost straight, keeping the constant value of prescribed normal stress. In the case of the NCP test, the normal stress increases before the shear stress reaches a well defined peak value (see also Fig. 5). After the peak, the shear stress decreases under almost constant normal stress, and then the stress path moves to the lower left showing an almost constant stress ratio of  $\tau/\sigma$ . In this paper, the stress state mentioned above will be called the residual state. Although the stress paths for different test conditions (CP and NCP) are different as shown in Fig. 4, the stress ratios  $\tau/\sigma$  at the peak or residual state almost coincide with each other. Therefore, the same strength parameters are given from both types of direct box shear tests (CP and NCP) on soil-geogrid. It has been confirmed that the same trend is obtained from test results on soil specimens alone, provided that the normal stress is measured at the opposite side of the loading system (JGS 0561-2000). Angles of shear resistance ( $\phi_{max}$ ,  $\phi_r$ ) and co-

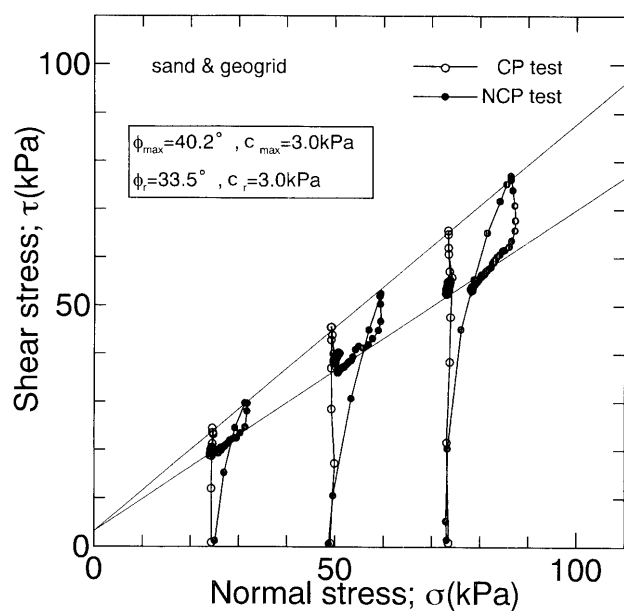


Fig. 4. Effect of the difference of normal stress loading method on the stress paths (DBS test)

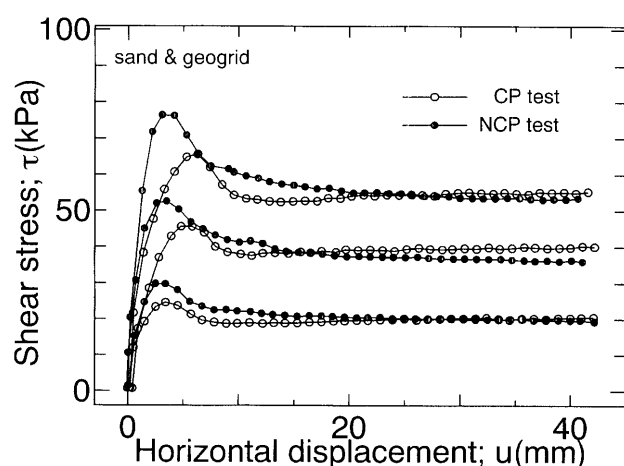


Fig. 5. Effect of the difference of normal stress loading method on the shear stress vs. horizontal displacement relationships (DBS test)

hesion intercepts ( $c_{\max}$ ,  $c_r$ ) obtained from these tests are shown in Fig. 4. The shear stress vs. horizontal displacement relationships obtained by the tests mentioned above are shown in Fig. 5. In the case of the CP test, horizontal displacements corresponding to the peak shear stresses are larger than those obtained by the NCP test. Larger peak shear stress of NCP test than that of CP test is due to the increase of normal stress before the shear stress reaches the peak value in the NCP test (Fig. 4). Residual state strength parameters ( $c_r$ ,  $\phi_r$ ) and horizontal displacement, corresponding to the peak shear stress obtained by CP tests, are used later in this paper to estimate the in-soil behavior of geogrid, compared with the pull-out test results.

#### Pull-Out Testing Method

An outline of the pull-out test apparatus used in this

paper is shown in Fig. 6. A pull-out box is used with inner dimensions of 220 mm width, 500 mm length and 200 mm depth. Each dimension is slightly smaller than those recommended by JSF T941-1994 (draft). The inside walls of the box are lubricated by latex membranes with grease for reducing the effect of friction between the soil specimen and the wall of the pull-out box. The pull-out opening arranged at the mid-height of the front wall was designed so that its opening size ( $t$ ) could be changed up to 8 mm in accordance with the thickness of geogrid specimen (Fig. 7). Sand and geogrid specimens used for the pull-out tests were the same as those used for DBS tests. Yufutsu sand was prepared in the pull-out box by the same method (multiple sieve pluviation method) used in the DBS test. The same type of geogrid used in the DBS test is buried at the mid-height of the pull-out box. The end of six inextensible wires are bound to the nodes of the geogrid, the spacings of which are about 125 mm and one of them is located outside of the pull-out box. The other end of the wires is led out from the rear wall for measuring the displacement of the geogrid by LVDT. Wires are passed through the flexible tube for reducing the effect of the friction between sand and wires. The normal stress is loaded at the top of the pull-out box using a rubber membrane with air pressure (25, 49, 74 kPa). The rate of pull-out displacement is 1 mm/min at the cramp jointed at the front end of the geogrid. In the test condition where the geogrid end is fixed, the geogrid is bound to the rear wall of the pull-out box with a steel plate. For investigating the effect of an embedded length of geogrid, pull-out tests with three kinds of geogrid length (250, 375, 500 mm) were carried out. The pull-out displacement ( $D$ ) is measured at the node located near the front wall in the initial stage of pull-out loading. Since the node moves gradually away from the pull-out box as the pull-out test progresses, the strain of the part of the geogrid existing outside of the box is accumulated as an error. Therefore, the pull-out displacement is modified with the following expression.

$$D = d - (d + d_i) \times f/S \quad (1)$$

where,  $d$  (mm) is the measured value of pull-out displacement,  $f$  (kN/m) is the pull-out force per unit width and  $S$  (kN/m) is the stiffness of geogrid. For reasons of the spacing size of geogrid ribs and the length of pull-out box, the end of the inextensible wire, it may not be possible to bind it to the node just at the location of the pull-out opening. The distance from the pull-out opening to the node where the end of the wire is bound is denoted as  $d_i$  (the initial value of pull-out displacement shown in Fig. 8).

#### Preliminary Test Results of the Pull-Out Test Examining the Influence of the Size of the Pull-Out Opening

A series of pull-out tests changing the size of the pull-out opening ( $t$  in Fig. 7) to 4, 6 and 8 mm were performed as preliminary tests. The pull-out force vs. pull-out displacement relationships obtained by the tests mentioned above are shown in Fig. 9. When the ribs of geogrid with

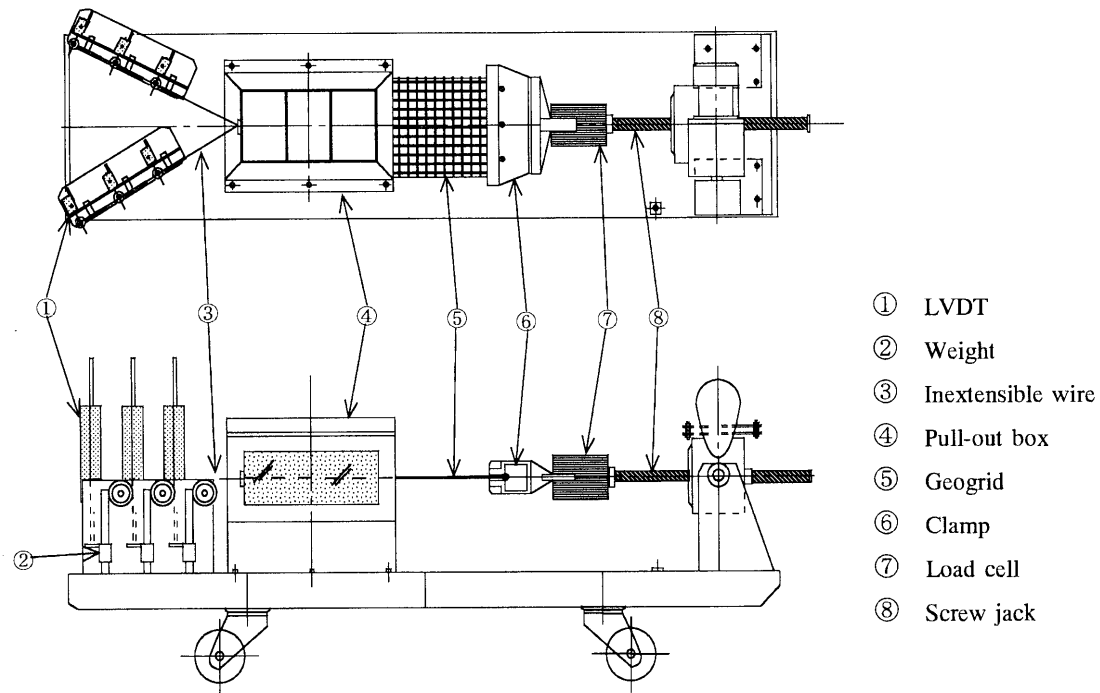


Fig. 6. Pull-out test apparatus

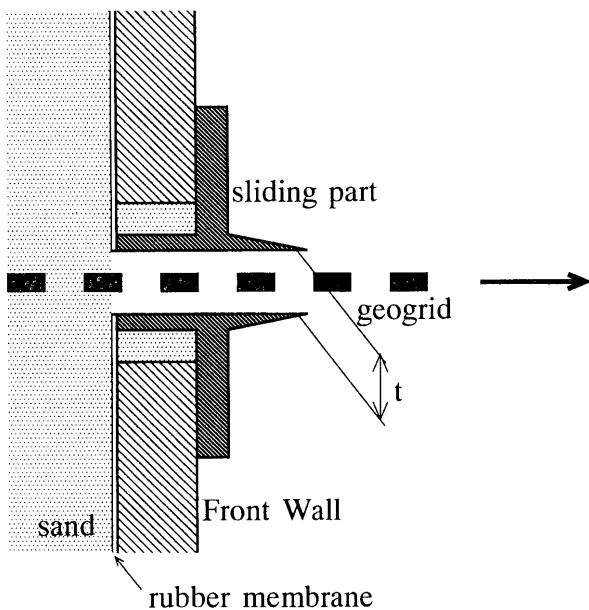
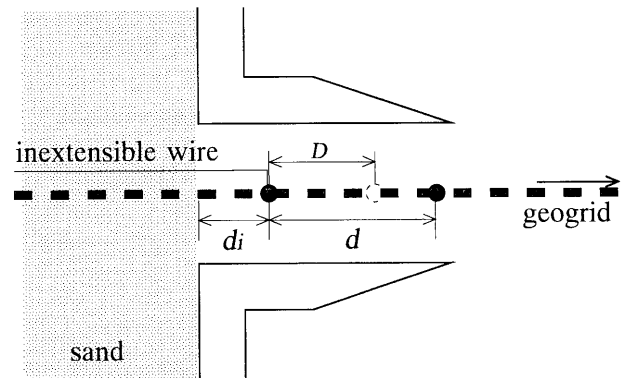


Fig. 7. Configuration of pull-out opening

Fig. 8. Definition of  $D$ ,  $d$  and  $d_i$  in Eq. (1)

sand particles pass through the opening of the pull-out box, the pull-out force temporarily decreases but then is recovered soon with the progression of the pull-out displacement. As a result, the unevenness of the pull-out force vs. pull-out displacement curve after the peak is seen in Fig. 9. When the normal stress level is low, no effect of the size of the pull-out opening is seen in this figure. For high normal stress level, the pull-out force is smaller when the pull-out opening is made at the maximum size (8 mm). The reasons for this tendency are inferred as follows. The higher the normal stress level, a

larger pull-out displacement corresponding to the peak pull-out force is needed. According to this, normal stress is decreased due to the phenomenon of sand particles in the vicinity of the pull-out opening being forced out of the pull-out box during the test, which causes the pull-out force to be decreased. The phenomenon described above will be even more marked for larger sizes of pull-out openings. In addition to this, the validity of the inference mentioned above is proved by the observation that more sand particles are forced out when the pull-out opening is 8 mm. Based on the results shown above, the optimal size of the pull out opening was adopted as 4 mm (twice as thick as the ribs) in this paper.

#### ESTIMATING METHOD FOR IN-SOIL DEFORMATION BEHAVIOR OF GEOGRID

Based on the results of DBS tests, the shear stress vs.

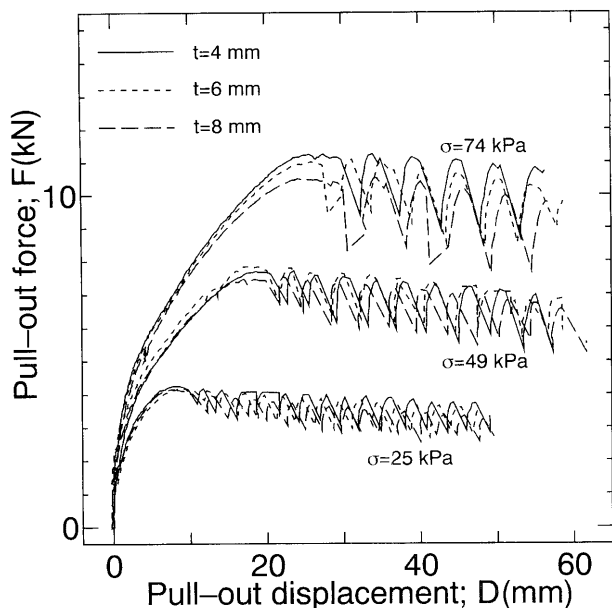


Fig. 9. Effects of pull-out opening size on the pull-out force vs. pull-out displacement relationships (pull-out test)

relative displacement relationship between soil and geogrid developed in the reinforced soil element is simply assumed to be as in Fig. 10. Referring to the reinforced soil element in Fig. 11, the shear stress acting along a geogrid is imagined to be transmitted toward the geogrid end in the soil during pull-out loading and distributed as shown in Fig. 11. Assuming that the tensile force vs. strain relationship of geogrid is represented as linear having the stiffness  $S$ , and combining the assumptions illustrated in Figs. 10 and 11, the following differential equations expressed by the variables of relative displacement between soil and geogrid ( $u$ ) and the distance from the in-soil end of geogrid ( $x$ ) are obtained (Mitachi et al., 1992).

$$\frac{d^2u}{dx^2} = \frac{2k}{S} u \quad (u \leq u_p) \quad (2)$$

$$\frac{d^2u}{dx^2} = \frac{2\tau_r}{S} \quad (u > u_p) \quad (3)$$

where,  $k = \tau_r / u_p$ , and  $\tau_r$  and  $u_p$  are the residual shear strength and the relative displacement corresponding to  $\tau_r$  in Fig. 10, respectively.

The distance from the in-soil end of geogrid ( $x$ ) is assumed to be  $x_p$ , where the relative displacement between soil and geogrid ( $u$ ) is equal to  $u_p$ . The distribution of relative displacement ( $u$ ), shear stress ( $\tau$ ) and tensile force ( $T$ ) developed along an in-soil geogrid can be obtained considering the two zones of  $x$ , namely ( $0 \leq x \leq x_p$ ) and ( $x \geq x_p$ ). Considering the case where geogrid material is used in the field without fixing its in-soil end, or the case in conventional pull-out tests, the restraint condition of the geogrid end is free (Fig. 12). On the other hand, considering the case where the in-soil end of geogrid is fixed such as with a wooden stake, for reducing the slackening

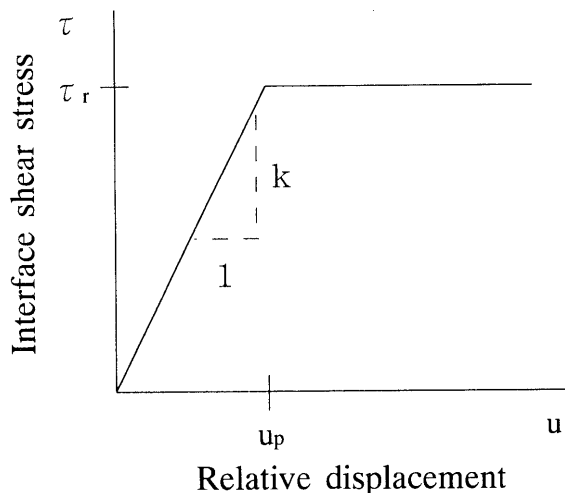


Fig. 10. Assumption of the shear stress vs. relative displacement relationship between soil and geogrid in the element

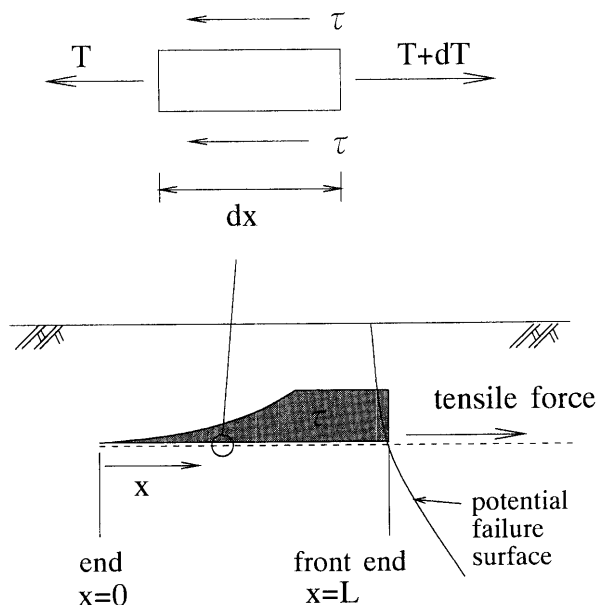


Fig. 11. Schematic representation on the distribution of the shear stress along the reinforced soil element

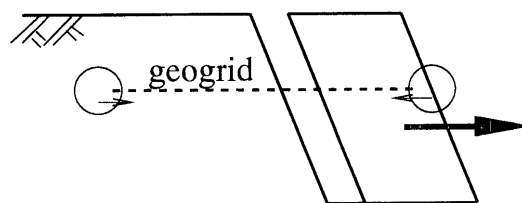


Fig. 12. Schematic representation on the "free end" condition

of geogrid, or the case of making a stability calculation of a half part of the embankment when the geogrid is embedded over the whole section of the embankment, the restraint condition of geogrid may be regarded as fixed. In the case of a construction method where the front end of the geogrid is fixed to a slope protector like a soil block

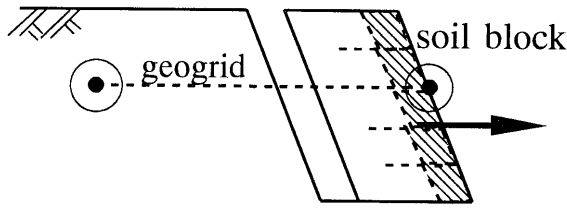


Fig. 13. Schematic representation on the "fixed end" condition

or steel frame, the restraint condition of geogrid end at the slope side is considered to be fixed as schematically shown in Fig. 13, in which the pull-out phenomenon in the sliding soil mass is considered. Boundary conditions of differential Eqs. (2) and (3) should be changed according to the restraint conditions of geogrid end mentioned above.

1) In the case of free end

for the zone ( $0 \leq x \leq x_p$ ):

Solving Eq. (2), by applying the boundary condition ( $x=0: du/dt (= \varepsilon) = 0$  and  $x=x_p: u = u_p$ ), the following Eqs. (4) can be obtained.

$$u = \frac{u_p}{\cosh(ax_p)} \cosh(ax) \quad (4-1)$$

$$\tau = \frac{ku_p}{\cosh(ax_p)} \cosh(ax) \quad (4-2)$$

$$T = \frac{2ku_p}{a \cosh(ax_p)} \sinh(ax) \quad (4-3)$$

$$a = \sqrt{2k/S} \quad (4-4)$$

for the zone ( $x \geq x_p$ ):

Solving Eq. (3), by applying the boundary condition ( $x=x_p: u = u_p, T = T_p$ ), the following Eqs. (5) can be obtained.

$$u = \frac{\tau_r}{S} (x - x_p)^2 + \frac{T_p}{S} (x - x_p) + u_p \quad (5-1)$$

$$T = T_p + 2\tau_r(x - x_p) \quad (5-2)$$

$$T_p = \frac{2ku_p}{a} \tanh(ax_p) \quad (5-3)$$

where  $T_p$  is the tensile force at  $x = x_p$ .

2) In the case of fixed end

for the zone ( $0 \leq x \leq x_p$ ):

Solving Eq. (2), by applying the boundary condition ( $x=0: u=0, T=T_0$  and  $x=x_p: u=u_p$ ) the following Eqs. (6) can be obtained.

$$u = \frac{u_p}{\sinh(ax_p)} \sinh(ax) \quad (6-1)$$

$$\tau = \frac{ku_p}{\sinh(ax_p)} \sinh(ax) \quad (6-2)$$

$$T = T_0 + \frac{2ku_p}{a \sinh(ax_p)} (\cosh(ax) - 1) \quad (6-3)$$

$$T_0 = \frac{au_p S}{\sinh(ax_p)} \quad (6-4)$$

where  $T_0$  is the tensile force at the fixed end ( $x=0$ ).

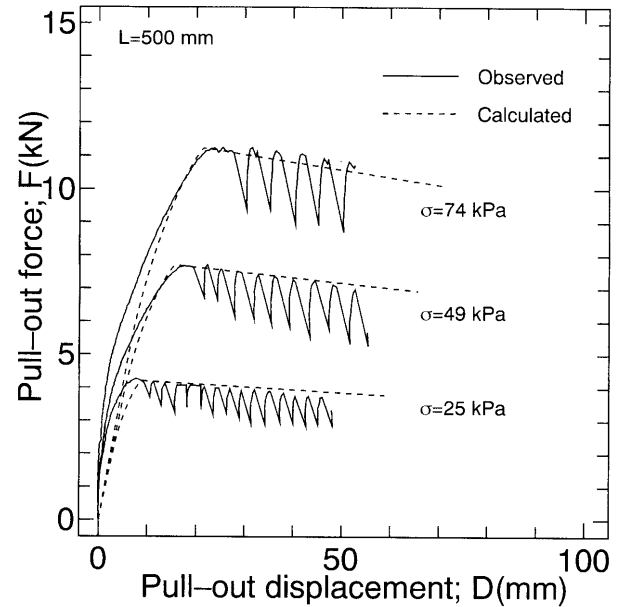


Fig. 14. Comparisons between calculated and observed pull-out force vs. displacement relationships (free end,  $L = 500$  mm)

for the zone ( $x \geq x_p$ ):

Solving Eq. (3), by applying the boundary condition ( $x=x_p: u = u_p, T = T_p$ ) the following Eqs. (7) can be obtained.

$$u = \frac{\tau_r}{S} (x - x_p)^2 + \frac{T_p}{S} (x - x_p) + u_p \quad (7-1)$$

$$T = T_p + 2\tau_r(x - x_p) \quad (7-2)$$

$$T_p = T_0 + \frac{2ku_p}{a \sinh(ax_p)} (\cosh(ax_p) - 1) \quad (7-3)$$

## COMPARISONS OF CALCULATED PULL-OUT FORCE VS. PULL-OUT DISPLACEMENTS WITH EXPERIMENTAL RESULTS

### In the Case of Free End

The pull-out force vs. pull-out displacement relationships calculated by the estimating method mentioned above, using the parameters ( $c_r = 3.0$  kPa,  $\phi_r = 33.5^\circ$ ,  $u_p = 3, 5, 6$  mm) obtained from the results of soil-geogrid DBS tests, are compared with those obtained by a series of pull-out tests. The comparisons are shown in Fig. 14. Pull-out tests were performed while changing the magnitude of normal stress as three under the condition that the embedded length and width of geogrid were 500 mm and 220 mm, respectively. The width of the geogrid was equal to that of the pull-out apparatus. This figure shows that calculated peak pull-out forces, displacements corresponding to the peak pull-out forces and residual pull-out forces almost coincide with the observed ones in every normal stress. On the other hand, observed pull-out force vs. pull-out displacement relationships at the early stage of pull-out test are plotted to the left of the calculated ones. The difference of the calculated and observed relationships originates from the measuring time lag

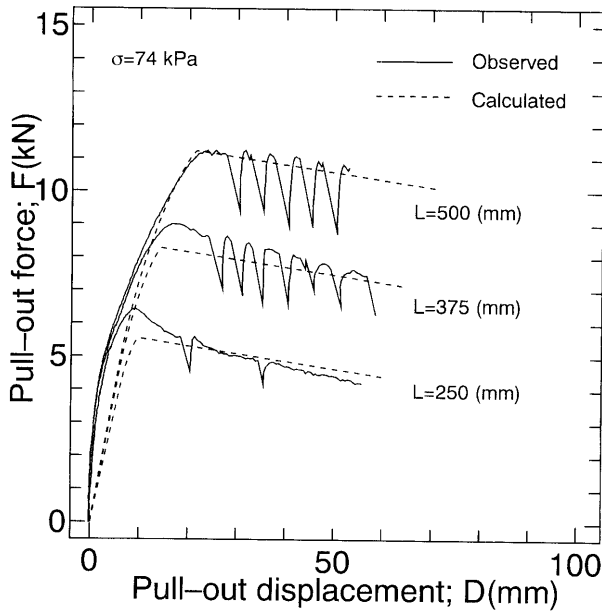


Fig. 15. Comparisons between calculated and observed pull-out force vs. displacement relationships (free end,  $\sigma = 74$  kPa)

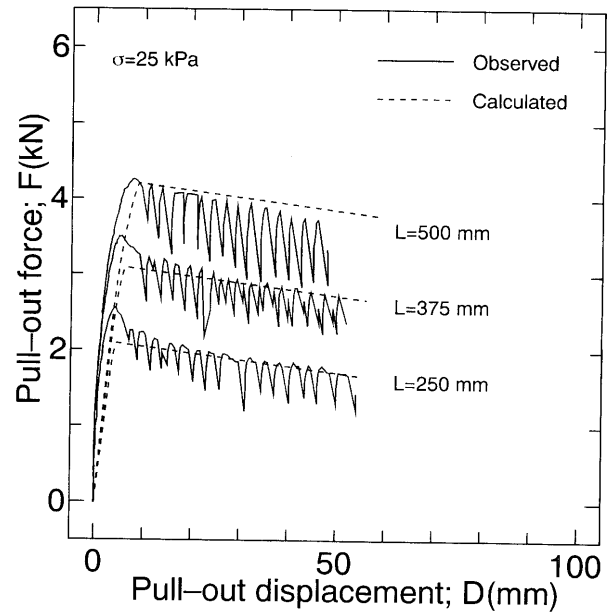


Fig. 17. Comparisons between calculated and observed pull-out force vs. displacement relationships (free end,  $\sigma = 25$  kPa)

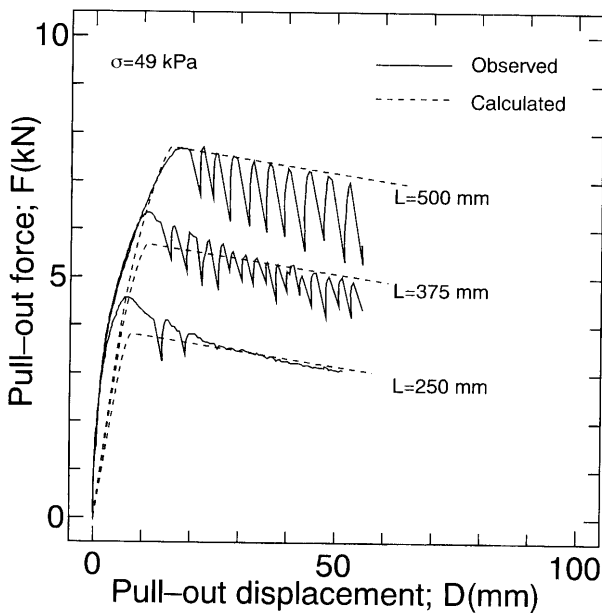


Fig. 16. Comparisons between calculated and observed pull-out force vs. displacement relationships (free end,  $\sigma = 49$  kPa)

caused by local deformation of the geogrid nodes to which the inextensible wires are bound. In addition to this, a larger pull-out force than actually exists may be measured due to the arch action developed in the vicinity of the pull-out opening caused by the existence of the front wall of the pull-out box.

Comparisons between calculated and pull-out test results changing the embedded length of geogrid are shown in Figs. 15, 16 and 17 separately by each normal stress. When the normal stress is 74 kPa (Fig. 15), calculated residual pull-out forces almost coincide with the observed ones; but, when the embedded length is short, cal-

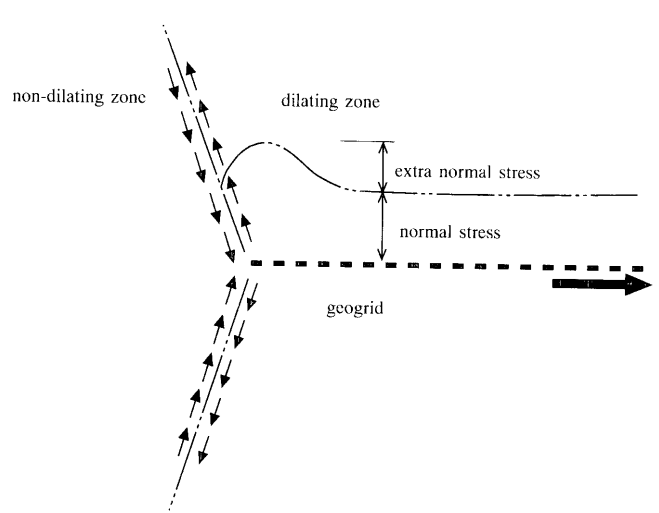


Fig. 18. Dilating zone and non-dilating zone in the vicinity of geogrid end

culated peak pull-out forces are smaller than observed ones. The reason for this tendency may be explained as follows. In the case that the embedded length is shorter than the length of the pull-out box, excessive normal stress may be exerted in the vicinity of the geogrid end as shown in Fig. 18 due to friction between the dilating zone developed by the displacement of soil-geogrid and non-dilating zone where a geogrid does not exist. The phenomenon mentioned above has been previously reported, and occurs in the case where the width of geogrid specimen is narrower than the pull-out box (Hayashi et al., 1996). Considering the overestimation of the pull-out force caused by the excessive normal stress mentioned above, calculated and observed pull-out force vs. pull-out displacement relationships may almost coin-

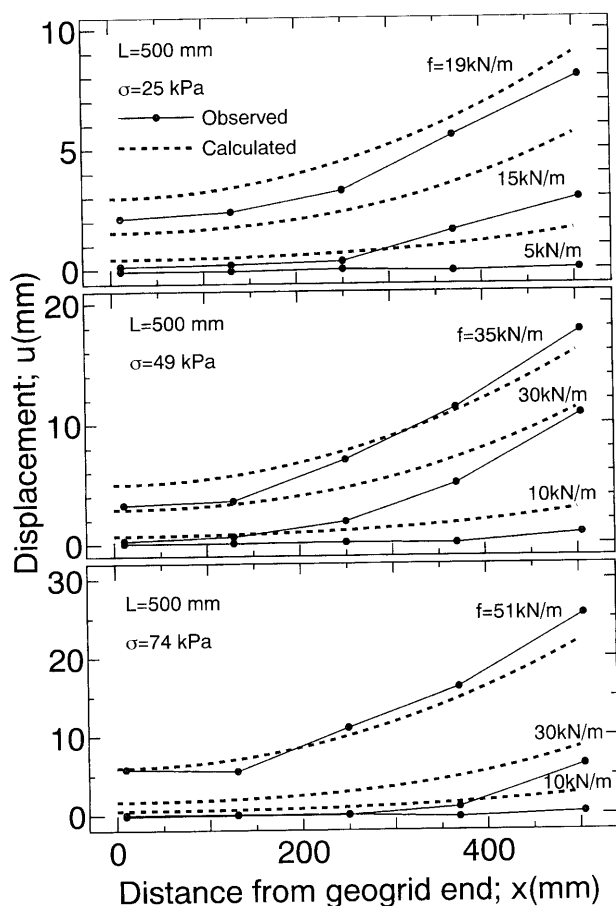


Fig. 19. Comparisons between calculated and observed distributions of in-soil displacement of geogrid (free end)

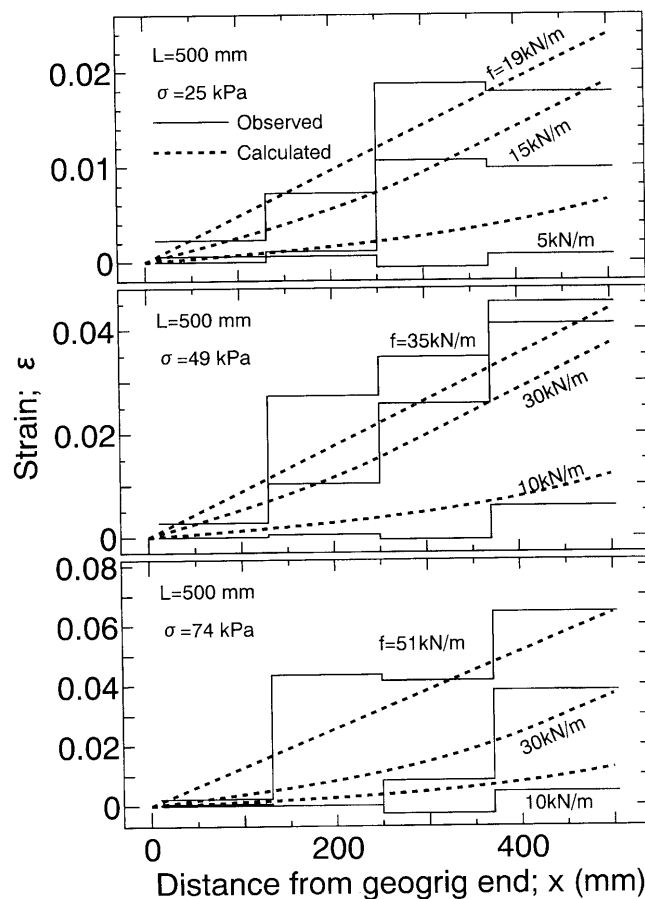


Fig. 20. Comparisons between calculated and observed distributions of in-soil strain of geogrid (free end)

side with each other. In order to verify the above-mentioned error caused by excessive normal stress, it is necessary to perform a series of pull-out tests changing the length of the pull-out box. Therefore, the size of the geogrid specimen has to be set equal to the inner size of the pull-out box. The pull-out force vs. pull-out displacement relationships before the peak shown in Fig. 15, display the same trend as illustrated in Fig. 14, and the same explanation as mentioned for Fig. 14 could be applied for this case as well. In the case where normal stresses are 25 and 49 kPa (Figs. 16 and 17), a similar trend to those mentioned in Fig. 15 can be seen. As described above, the method for estimating the in-soil deformation behavior of geogrid based on the results of DBS tests can be successfully applied to predict the pull-out test results in any case where changing the embedded length as well as normal stress is changed. Consequently, it is possible to estimate precisely the in-soil deformation behavior of geogrid in the field without performing laborious full-scale pull-out tests.

Comparisons of calculated and observed in-soil displacements and strains in the case, here the embedded length of geogrid is 500 mm are shown in Figs. 19 and 20. The maximum values of pull-out force per unit width ( $f$ ) in these figures correspond to the peak pull-out forces in each case of the pull-out test in Fig. 14. As the pull-out

force increases with the progression of the pull-out test, calculated values become closer to the observed ones. On the other hand, at the initial stage of the pull-out test, calculated results are larger than observed ones. This tendency is clearer in the vicinity of the in-soil end of geogrid. As mentioned in relation to Fig. 14, the displacement of geogrid is restricted due to the arch action developed in the vicinity of the pull-out opening, the pull-out force is not fully transmitted to the interior part of the pull-out box, and hence smaller displacement is measured. According to the strain distributions illustrated in Fig. 20, the observed tensile strains of geogrid in the vicinity of the pull-out opening are smaller than calculated ones. In relation to this, the influence of the arch action due to the existence of the front wall of the pull-out box is recognized again. The lower the normal stress, the clearer the influence of arch action on the observed strain magnitude, and hence the difference between the observed and calculated results becomes larger.

#### *The Effect of the Restraint Conditions of Geogrid End*

The pull-out force vs. pull-out displacement relationships obtained by a series of pull-out tests, in which the end of geogrid is fixed to the rear wall of the pull-out box (fixed end condition) or not fixed (free end condition), are shown in Fig. 21. In the test series, the embedded length

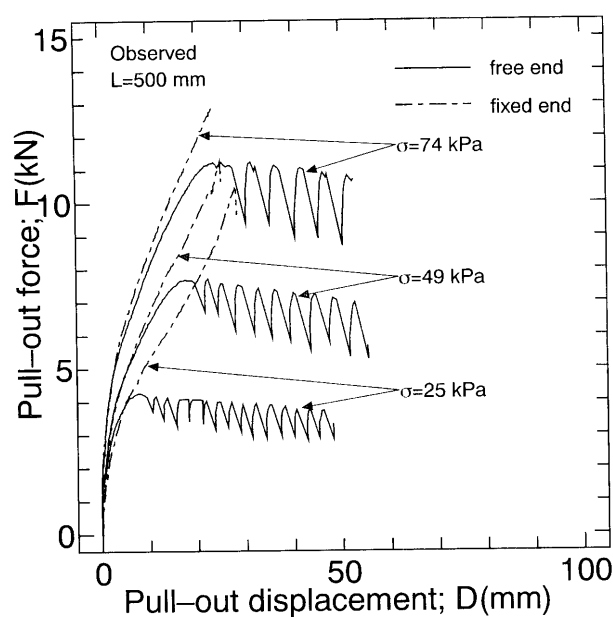


Fig. 21. Effects of restraint conditions of geogrid end on the pull-out force vs. pull-out displacement relationships (pull-out test)

of geogrid is 500 mm, and normal stresses are 25, 49 and 74 kPa. In the case of a fixed end, the pull-out resistance increases up to the material tensile strength at which point the geogrid is broken down without showing the residual state (pull-out off of the geogrid) like in the case of the free end. In this test program, pull-out tests could not be performed up to the material tensile strength owing to the limit of LVDT's stroke. It can also be seen from the figure that the higher the normal stress, a larger pull-out force is given with a small pull-out displacement. Especially in the initial stage of the pull-out test, the pull-out behavior is not influenced by the restraint conditions of the geogrid end. Calculated results on the same conditions as those in the pull-out tests mentioned above are shown in Fig. 22. In this figure, the same trend as illustrated in Fig. 21 is seen. It is concluded from these two figures that even if the end of the geogrid is fixed, it is impossible to reduce the initial displacement of geogrid without developing a full frictional resistance between soil and geogrid.

Comparisons of the calculated pull-out force vs. pull-out displacement relationships with the observed ones for the case of fixed end condition are shown in Fig. 23. Similar to the free end condition previously shown in Fig. 14, observed pull-out force vs. pull-out displacement relationships at the early stage of pull-out test are plotted at the left of the calculated ones owing to the own error of the pull-out test. This figure also shows that the observed pull-out force vs. pull-out displacement curves move to the right, across the calculated curves, after some amount of displacement, depending on the magnitude of normal stress. After this point, the observed curves deviate from the calculated ones. The reasons for the experimental results mentioned above are considered as follows. Calculations are performed under the assumption that the

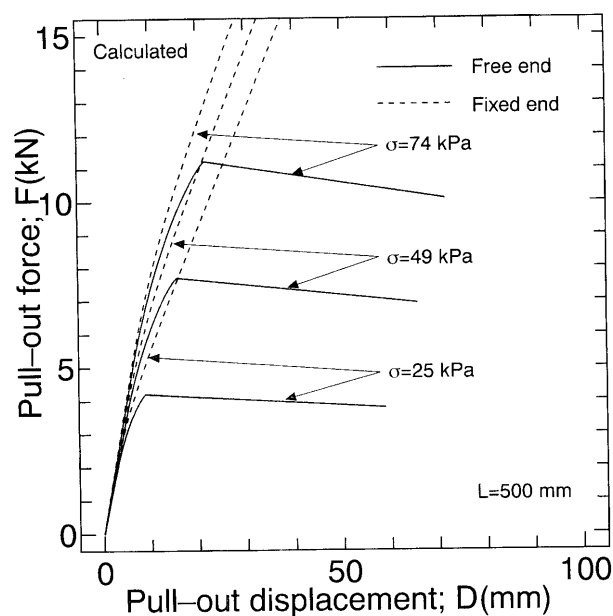


Fig. 22. Effects of restraint conditions of geogrid end on the pull-out force vs. pull-out displacement relationships (calculated)

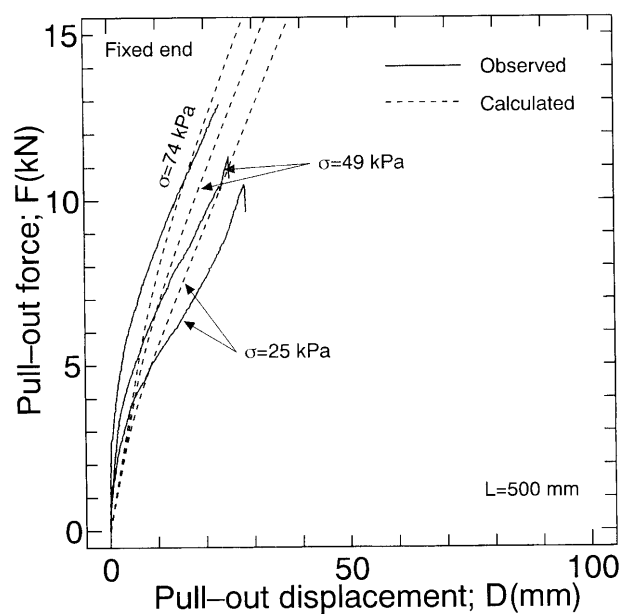


Fig. 23. Comparisons between calculated and observed pull-out force vs. displacement relationships (fixed end)

end of the geogrid is completely fixed; however, the restraint condition of geogrid end in pull-out tests is not completely fixed since the end of the geogrid is slightly moved (about 10 mm) due to the development of tensile force during the pull-out test. Moreover, since the pull-out displacement is measured at the geogrid node in the vicinity of the pull-out opening, which is moved out of the pull-out box, the creep deformation of geogrid is not negligible. This is also confirmed from the fact that the increase of pull-out displacement becomes significant when the pull-out force becomes larger.

Comparisons of distributions of in-soil geogrid dis-

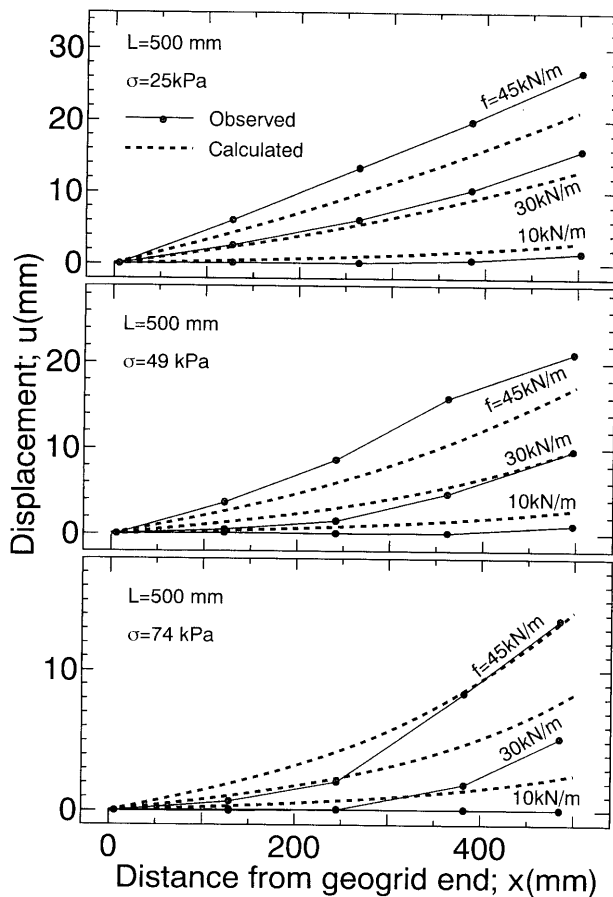


Fig. 24. Comparisons between calculated and observed distributions of in-soil displacement of geogrid (fixed end)

placement between observed and calculated results are shown in Fig. 24. Considering that the end of geogrid can not be fixed completely as mentioned above, the abscissa in the figure represents the distance from the end of the geogrid, namely the value obtained by subtracting the displacement of geogrid end from the displacement of each node of geogrid. As the pull-out force increases, both observed and calculated distribution curves of in-soil geogrid displacement become straight when the normal stress level is low ( $\sigma = 25$  kPa). When the stress level is high ( $\sigma = 74$  kPa), the slope of both observed and calculated distribution curves of in-soil geogrid displacement increase rapidly and become straight in the vicinity of the pull-out opening with the increase of pull-out force. According to this, it is clear that the greater part of the pull-out load is resisted by the geogrid, which is in the vicinity of the pull-out opening. The larger values of the observed displacement than those of calculated are obtained in the vicinity of the pull-out opening. This is due to the effect of creep deformation of geogrid mentioned above in relation to Fig. 23. Similar to the results of the free end condition mentioned above, the pull-out force is not fully transmitted to the interior part of the pull-out box, and hence smaller displacement than that obtained by calculation is measured for a high stress level ( $\sigma = 74$  kPa).

Comparisons of observed strain distributions of in-soil

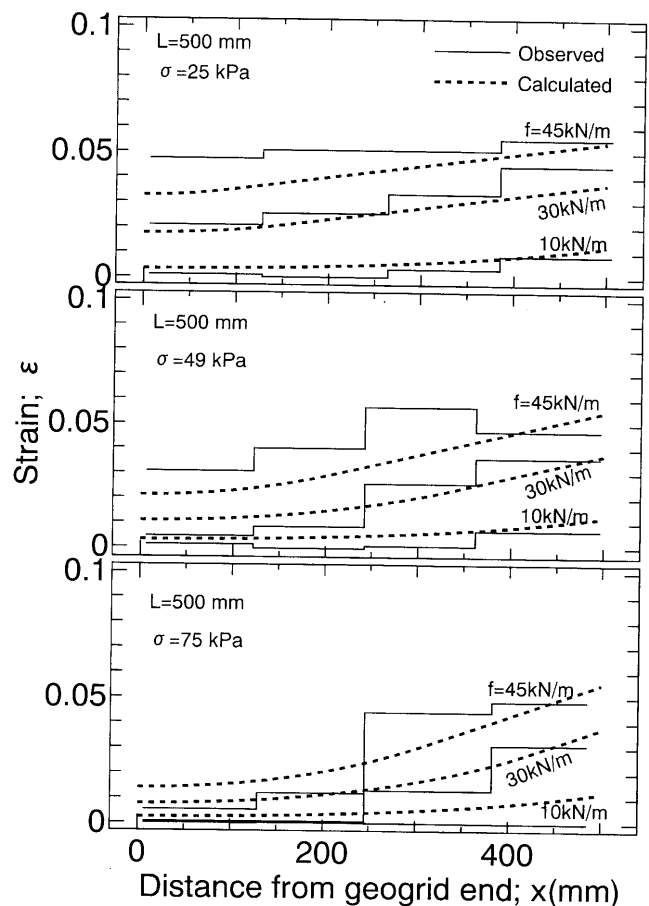


Fig. 25. Comparisons between calculated and observed distributions of in-soil strain of geogrid (fixed end)

geogrid with those calculated are shown in Fig. 25. When the stress level is high ( $\sigma = 74$  kPa), the strain is not fully transmitted to the interior part of the pull-out box irrespective of the increase of the pull-out force. On the other hand, when the stress level is low ( $\sigma = 25$  kPa), the large strains are developed at the interior part of the pull-out box with an increase in pull-out force. As a whole, calculated strain distributions are approximate to those observed by pull-out tests.

As mentioned above, taking account of the errors of a pull-out test own (the arch action originating from the existence of the front wall, the phenomenon of sand particles being forced out of the pull-out opening and the creep deformation of geogrid etc.) calculations of in-soil deformation behavior of geogrid for the case of pull out loading under various conditions by using the parameters obtained from DBS tests are quite reasonable. Therefore, the proposed method in this paper can be successfully used to estimate in-soil deformation behavior of geogrid and it is also suggested that it is important to establish a design method considering not only the deformation of geogrid itself, but the overall deformation of the reinforced soil structure which results from the in-soil deformation behavior of geogrid.

## CONCLUSIONS

Based on a series of direct box shear (DBS) tests changing the normal stress condition (controlling the normal stress to be constant and nominally constant without control) and a series of pull-out tests changing the restraint condition of geogrid end, the following conclusions were obtained.

- 1) Strength parameters corresponding to the peak or the residual states obtained from the two types of direct box shear tests almost coincide with each other.
- 2) In the case where the pull-out opening is large, the pull-out force decreases on account of the sand particles being forced out of the box. Consequently, it is important to adopt a suitable space of pull-out opening taking into account the thickness of geogrid specimen.

From the comparisons of calculated results simulating pull-out tests under various conditions using parameters obtained from the DBS test with the observed pull-out test results, useful knowledge on designing or constructing reinforced soil structures were obtained as follows.

- 3) Using the method proposed in this paper with the strength parameters obtained by DBS tests, it is possible to estimate in-soil behavior of geogrid under various conditions changing the embedded length of geogrid, magnitude of the normal stress, in-soil end restraint of geogrid and so on.
- 4) As the pull-out force vs. pull-out displacement relationships depend not on the conditions of in-soil end restraint of geogrid but on the normal stress exerted on the geogrid, it is important to construct a reinforced soil structure so that sufficient frictional resistance develops between soil and geogrid.

## REFERENCES

- 1) American Society for Testing and Materials (1993): Standard Test Method for Determining the Coefficient of Soil and Geosynthetic or Geosynthetic and Geosynthetic Friction by the Direct Shear Method, ASTM D 5321-92.
- 2) Bergado, D. T., Shivashankar, R., Alfaro, M. C., Chai, J. C. and Balasubramaniam, A. S. (1993): Interaction behavior of steel grid reinforcements in a clayey sand, *Géotechnique*, **43** (4), 589-603.
- 3) Hayashi, S., Alfaro, M. C. and Watanabe, K. (1996): Dilatancy effects of granular soil on the pullout resistance of strip reinforcement, *Proc. of the Int. Symp. on Earth Reinforcement*, Kyushu, Japan, **1**, 39-44, Balkema, Rotterdam.
- 4) Imaizumi, S., Takahashi, S., Yokoyama, Y. and Nishigata, T. (1995): Evaluation of pull-out behavior of HDPE geomembrane embedded in sand, *J. of Japanese Society of Civil Engineers*, (511/III-30), 155-162.
- 5) Ingold, T.S. (1983): A laboratory investigation of grid reinforcement in clay, *Geotech. Testing J.*, **6** (3), 112-119.
- 6) Japanese geotextile research group (2000): A manual of design and construct for geotextile reinforced soil (revised edition), *Public Works Research Center* (in Japanese).
- 7) Japanese Geotechnical Society (1994): Japanese Geotechnical Standard for Determination of Soil-Geotextile Frictional Behavior by Direct Shear Test and/or Pull-out Test, (draft) JSF T 941, *Tsuchi-to-Kiso*, **42** (1), 93-102 (in Japanese).
- 8) Japanese Geotechnical Society (2000): Japanese Geotechnical Standard on Method for Consolidated Constant Pressure Direct Box Shear Test on Soil, JGS T 561-2000.
- 9) Jewell, R. A. (1992): Links between the testing, modelling and design of reinforced soil, Keynote Lecture, *Proc. of the Int. Symp. on Earth Reinforcement*, Kyushu, Japan, **2**, 755-772, Balkema, Rotterdam.
- 10) Juran, I., Knochenmus, G., Acar, Y. B. and Arman, A. (1988): Pull-out response of geotextiles and geogrids (synthesis of available experimental data), *ASCE Special Publication*, **18**, 92-111.
- 11) Mitachi, T., Yamamoto, Y. and Muraki, S. (1992): Estimation of in-soil deformation behavior of geogrid under pull-out loading, *Proc. of the Int. Symp. on Earth Reinforcement*, Kyushu, Japan, **1**, 121-126, Balkema, Rotterdam.
- 12) Nakamura, T., Mitachi, T. and Ikeura, I. (1999): Direct shear testing method as a means for estimating geogrid-sand interface shear-displacement behavior, *Soils and Foundations*, **39** (4), 1-8.
- 13) Palmeira, E. M. and Milligan, G. W. E. (1989): Scale and other factors affecting the results of pull-out tests of grids buried in sand, *Géotechnique*, **39** (3), 511-524.